

## Butterfly Floquet Spectrum in Driven SU(2) Systems

Jiao Wang<sup>1,2</sup> and Jiangbin Gong<sup>3,4,\*</sup>

<sup>1</sup>Temasek Laboratories, National University of Singapore, 117542, Singapore

<sup>2</sup>Department of Physics, Institute of Theoretical Physics and Astrophysics, Xiamen University, Xiamen 361005, China

<sup>3</sup>Department of Physics and Center of Computational Science and Engineering, National University of Singapore, 117542, Singapore

<sup>4</sup>NUS Graduate School for Integrative Sciences and Engineering, Singapore 117597, Singapore

(Received 29 December 2008; published 17 June 2009)

The Floquet spectrum of a class of driven SU(2) systems is shown to display a butterfly pattern with multifractal properties. The level crossing between Floquet states of the same parity or different parities is studied. The results are relevant to studies of fractal statistics, quantum chaos, coherent destruction of tunneling, and the validity of mean-field descriptions of Bose-Einstein condensates.

DOI: 10.1103/PhysRevLett.102.244102

PACS numbers: 05.45.Mt, 03.75.Lm

Hofstadter's butterfly spectrum of the Harper model [1] has attracted tremendous mathematical, theoretical, and experimental interest. For an arbitrary irrational value of one system parameter, the spectrum of the Harper model is a fractal, which has been strictly proved after decades of research on the "ten martini problem" [2]. As one important implication, a fractal butterfly spectrum suggests the closing of a quantum gap infinite times and hence the occurrence of infinite quantum phase transitions [3].

Early quantum chaos studies established that the Floquet (quasienergy) spectrum of periodically driven systems may display a fractal butterfly pattern as well [4,5]. However, the nature of the fractal Floquet spectrum is still poorly understood. Indeed, because the eigenphase of Floquet states is restricted to a range of  $2\pi$ , understanding a Floquet spectrum associated with an infinite-dimensional Hilbert space is subtle and challenging [6]. Furthermore, previous findings regarding the fractal Floquet spectrum were largely limited to the so-called kicked-Harper model (a driven version of the Harper model) [7–9] and its variant [5,9,10].

Because of vast interests in quantum control especially in dressed matter waves [11–14], there are now promising possibilities for the engineering and simulation of driven ultracold systems with a prescribed Floquet spectrum. In this Letter, we show that the Floquet spectrum of a deceptively simple class of SU(2) systems, constructed from a driven two-mode Bose-Einstein condensate (BEC), displays a butterfly pattern and possesses truly remarkable properties. For example, we show that with one certain system parameter fixed the overall butterfly pattern is insensitive to the number of bosons (denoted  $N$ ) in the BEC, but some detailed features depend on whether  $N$  is odd or even. We shall reveal that the found butterfly pattern contains many level crossings between states of different parities and thus many points of coherent destruction of tunneling (CDT) [15], with the total number of CDT points found to scale as  $\sim N^{3.0}$ . As an analog of first-order quantum phase transitions, we discover that the found butterfly

pattern also contains many level crossings between same-parity eigenstates. These results suggest that the class of driven SU(2) systems studied here may become a test bed for a number of research topics. Several specific applications of this work are also discussed.

Driven two-mode BEC systems were proposed before [13,16,17] to realize the well-known kicked-top model [18] in the quantum chaos literature. In its most general form, a driven two-mode Bose-Hubbard model can be written as

$$H = f(t)\hbar(a_1^\dagger a_2 + a_2^\dagger a_1) + g(t)\hbar(a_1^\dagger a_1 - a_2^\dagger a_2)^2, \quad (1)$$

where  $a_i$  and  $a_i^\dagger$  are the bosonic annihilation and creation operators, respectively, for the  $i$ th mode,  $f(t)$  describes the time-dependent tunneling rate between the two modes, and the  $g(t)$  term describes the self-interaction between same-site bosons, whose time dependence can be achieved by Feshbach resonance induced by a magnetic field. The total number of bosons  $N = a_1^\dagger a_1 + a_2^\dagger a_2$  is a conserved quantity, and the dimension of the Hilbert space is  $N + 1$ . Using the Schwinger representation of angular-momentum operators, namely,  $J_x = (a_1^\dagger a_2 + a_2^\dagger a_1)/2$ ,  $J_y = (a_2^\dagger a_1 - a_1^\dagger a_2)/(2i)$ , and  $J_z = (a_1^\dagger a_1 - a_2^\dagger a_2)/2$ , Eq. (1) reduces to

$$H = 2f(t)\hbar J_x + 4g(t)\hbar J_z^2. \quad (2)$$

Clearly, the dynamics is solely determined by the SU(2) generators  $J_x$ ,  $J_y$ , and  $J_z$ . The total angular-momentum quantum number  $J$  is given by  $J = N/2$ . The Hilbert space can be expanded by the eigenstates of  $J_z$ , denoted  $|m\rangle$ , with  $J_z|m\rangle = m|m\rangle$ . The population difference between the two modes is given by the expectation value of  $2J_z$ . If we exchange the indices of the two modes, then  $J_x$  is invariant,  $J_z \rightarrow -J_z$ , and as a result the Hamiltonian in Eq. (2) is unchanged. This reflects a parity symmetry of our model.

Consider then two specific forms of  $f(t)$  and  $g(t)$ . In the first case  $f(t) = \alpha/(2\tau)$  and  $g(t) = g_0 \sum_n [\delta(t - 2n\tau - \tau) - \delta(t - 2n\tau)]$ . The Floquet operator, i.e., the unitary evolution operator  $F$  from  $2n\tau + 0^+$  to  $(2n + 2)\tau + 0^+$ , is then given by

$$F = e^{i\eta J_z^2/2J} e^{-i\alpha J_x} e^{-i\eta J_z^2/2J} e^{-i\alpha J_x}, \quad (3)$$

where  $\eta = 4g_0N$ . Because the first two or the last two factors in Eq. (3) constitute the Floquet operator for a standard kicked-top model [18], our driven system here can be regarded as a “double-kicked-top model.” Alternatively, if we set  $g(t) = g_0/\xi$  and  $f(t) = \frac{\alpha}{2} \sum_n [\delta(t - n\tau) + \delta(t - n\tau - \xi)]$ , where  $\xi$  is the time delay between the two delta kicking sequences, then the associated propagator  $F'$  from  $n\tau - 0^+$  to  $(n+1)\tau - 0^+$  is given by

$$F' = e^{i\eta J_z^2/2J} e^{-i(4g_0\tau/\xi)J_z^2} e^{-i\alpha J_x} e^{-i\eta J_z^2/2J} e^{-i\alpha J_x}. \quad (4)$$

Under the special condition  $4g_0\tau/\xi = 2k\pi$  ( $8k\pi$ ) for integer  $J$  (half integer  $J$ ), where  $k$  is an integer, the factor  $e^{-i(4g_0\tau/\xi)J_z^2}$  is unity in the  $(2J+1)$ -dimensional Hilbert space, and hence  $F'$  becomes identical with  $F$ . Thus, there exist two different scenarios for realizing  $F$ , the key operator to be analyzed below.

In the  $|m\rangle$  representation, the third factor  $e^{-i\eta J_z^2/2J}$  of  $F$  equals  $e^{-i\eta m^2/2J}$ , which is a pseudorandom number for irrational  $\eta/J$ . The first factor of  $F$ , however, effectively induces a time reversal of the third factor and thus partially cancels this pseudorandom phase. Indeed, using the  $SU(2)$  algebra, the product of the first three factors of  $F$  in Eq. (3) is given by

$$e^{i\eta J_z^2/2J} e^{-i\alpha J_x} e^{-i\eta J_z^2/2J} = e^{-i\alpha[(J_x/2 + iJ_y/2)e^{i\eta(2J_z+1)/2J} + \text{c.c.}]}, \quad (5)$$

showing that the  $\eta$ -dependent term entering into  $F$  becomes  $e^{i[\eta(2J_z+1)/2J]}$ , which is always a quasiperiodic number  $e^{i[\eta(2m+1)/2J]}$  in the  $|m\rangle$  representation. This partial cancellation of quasirandom dynamical phases implies intriguing spectral properties [19].

To study the classical limit of  $F$ , we consider scaled variables  $x = J_x/J$ ,  $y = J_y/J$ , and  $z = J_z/J$ . The three operators  $x$ ,  $y$ , and  $z$  also satisfy the angular-momentum algebra but with an effective Planck constant  $\hbar_{\text{eff}} \equiv 1/J$ . By taking the  $\hbar_{\text{eff}} \rightarrow 0$  limit with fixed  $\eta$  and  $\alpha$ , the classical dynamics associated with  $F$  can be obtained, with variables  $x$ ,  $y$ , and  $z$  restricted on a unit sphere. Because  $\eta = 4g_0N$ , this classical limit with fixed  $\eta$  requires  $N \rightarrow +\infty$  and  $g_0 \rightarrow 0$ . This condition is apparently equivalent to that in a standard mean-field limit of the driven BEC.

Figure 1 shows the typical eigenphase spectrum of  $F$  vs  $\hbar_\eta \equiv \eta\hbar_{\text{eff}} = \eta/J = 8g_0$ , for  $J = 20, 20.5, 100$  and  $\alpha/\hbar_{\text{eff}} = 1.0$ . Because the spectrum of  $F$  is invariant if  $\hbar_\eta \rightarrow \hbar_\eta + 4\pi$ , we set  $\hbar_\eta \in [0, 4\pi)$ . Though in Fig. 1 the involved Hilbert space is rather small, spectacular butterfly patterns are already obtained (their symmetry with respect to  $\hbar_\eta = 2\pi$  can be proved). They resemble the famous Hofstadter's butterfly but also present remarkable differences in several aspects. First, if we take a vertical cut of the butterfly patterns in Fig. 1, the spectrum is not found to present any large gap. Second, the butterfly patterns shown

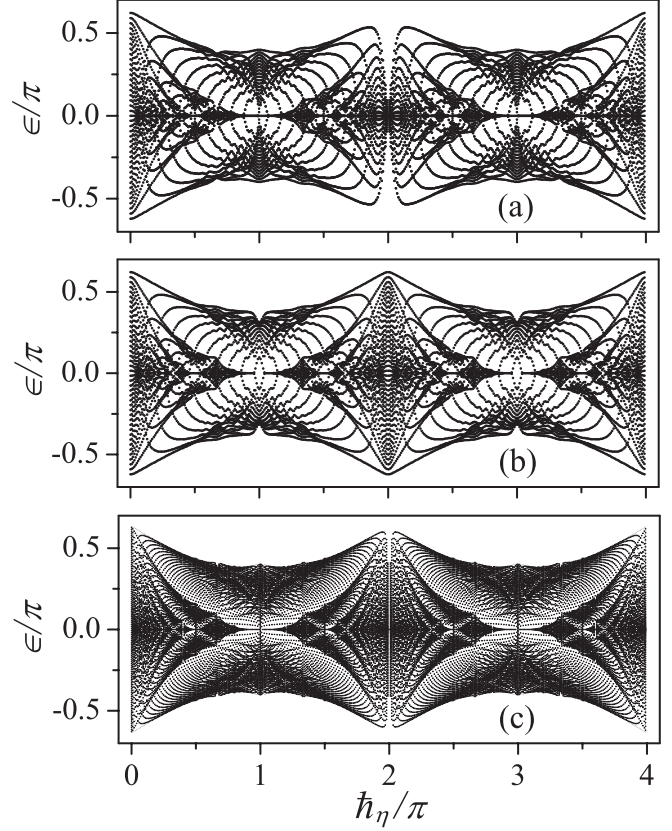


FIG. 1. Eigenphase spectrum (denoted  $\epsilon$ ) of the Floquet operator  $F$  in Eq. (3).  $J = 20$  in (a),  $20.5$  in (b), and  $100$  in (c).  $\alpha/\hbar_{\text{eff}} = \alpha J = 1.0$  in all panels.

in each panel of Fig. 1 possess a double-butterfly structure, with each butterfly covering a  $2\pi$  range of  $\hbar_\eta$ . This double-butterfly structure is somewhat analogous to the spectrum of a Harper-like effective Hamiltonian considered in Ref. [9]. More interestingly, though Fig. 1(c) has many more levels than Figs. 1(a) and 1(b), the overall outline of the double-butterfly structure is seen to be insensitive to  $J$  for fixed  $\alpha/\hbar_{\text{eff}} = \alpha J$ . For a fixed value of  $J$  but for other not too large values of  $\alpha$ , the qualitative features of the butterfly spectrum remain but at different scales. For very large values of  $\alpha$  (e.g.,  $\alpha/\hbar_{\text{eff}} > 10$ ), the butterfly pattern for a fixed value of  $J$  will gradually dissolve, in a similar fashion as in the kicked-Harper model [4].

Some detailed aspects of the spectrum are also noteworthy. For example, it is observed that the spectrum collapses to one point for  $\hbar_\eta = 2\pi$ , if and only if  $J$  is an integer. This can be explained as follows. If  $J$  is an integer and if  $\hbar_\eta = 2\pi$ , then in the  $|m\rangle$  representation,  $e^{-i\eta J_z^2/2J} = e^{-i\pi m^2} = e^{-i\pi m} = e^{-i\pi J_z}$ . So in this case  $e^{-i\eta J_z^2/2J}$  is equivalent to a rotation of  $\pi$  around the  $z$  axis, and hence the first three factors of  $F$  exactly cancel its last factor. This cancellation will not occur if  $J$  is a half integer, i.e., if  $N$  is odd.

Figure 2 depicts the phase space structure of the classical limit of  $F$ . As  $\eta$  increases, the classical dynamics changes

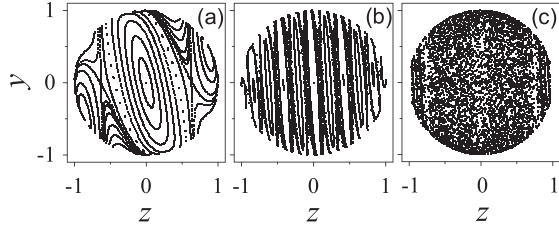


FIG. 2. Poincaré surfaces of a section (with  $J_x > 0$ ) of the classical or mean-field limit of  $F$  in Eq. (3), with  $\alpha = 0.05$  [the same as in Fig. 1(a)] and  $\eta = 5$  in (a), 30 in (b), and 75 in (c).

from being regular to being chaotic. On the other hand, the Floquet spectrum shown in Fig. 1 can be, however, very similar for radically different values of  $\eta$  ranging from 0 to  $4\pi/\hbar_{\text{eff}} = 4J\pi$ . Therefore, upon quantization the regular or chaotic nature of the classical dynamics might not necessarily be reflected in the spectrum and hence can be irrelevant to the quantum dynamics.

The statistical behavior of the found butterfly spectrum is also examined. To have good statistics we consider a much larger value of  $J$ . Figure 3(a) presents the cumulative level density  $N(\epsilon)$  for a representative value of  $\hbar_\eta$ .  $N(\epsilon)$  is highly irregular but does not show any clear flat steps. This is consistent with our early observation that no large gap exists in the spectrum. Figures 3(b)–3(d) show the associated level distribution  $P(\epsilon)$  at three different scales. Evidently,  $P(\epsilon)$  has a fascinating self-similar property.

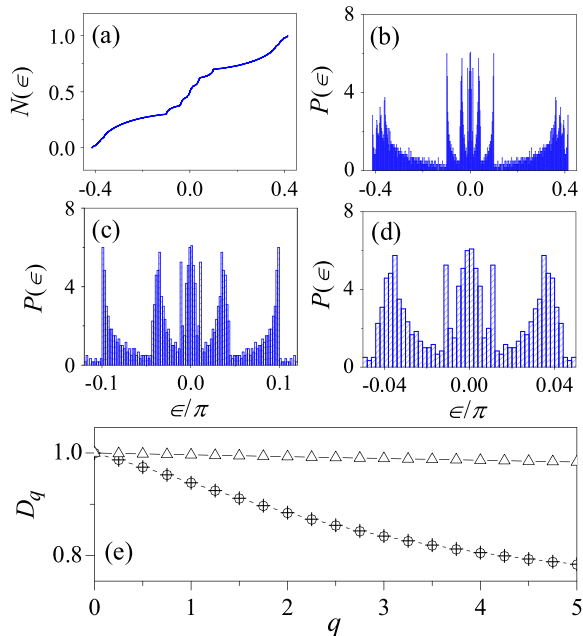


FIG. 3 (color online). (a) The cumulative Floquet state density and (b)–(d) the Floquet state density distribution at different scales, for  $\hbar_\eta = (\sqrt{5} - 1)\pi/2$ ,  $\alpha/\hbar_{\text{eff}} = 1$ , and  $J = 2999$ . Panel (e) shows the generalized fractal dimension  $D_q$ . Crosses and circles are for odd-parity and even-parity states, respectively. Triangles represent the result for a standard kicked-top model.

This motivates us to quantitatively characterize the spectrum via the generalized fractal dimension  $D_q$ , with the results shown in Fig. 3(e). As expected from the  $N(\epsilon)$  result in Fig. 3(a),  $D_0 = 1$ . However,  $D_q$  for  $q \neq 0$  clearly shows that the spectrum has multifractal properties. For comparison, Fig. 3(e) also shows the  $D_q$  result for a standard kicked-top model with the same values of  $\eta$  and  $\alpha$  (i.e., considering an operator comprising only the first two factors of  $F$ ). The  $D_q$  behavior in the kicked-top case is as trivial as that of a random sequence: It remains close to unity and slightly decreases with increasing  $q$  due to finite-size effects. Based on these results, we conjecture and invite a formal mathematical proof that the butterfly patterns found here contain true fractals in the limit of  $J \rightarrow +\infty$ .

We next study the level crossings in the butterfly patterns. Interestingly, the minimal distance in  $\hbar_\eta$  between two level crossings is found to decrease sharply with  $J$ . So even for a rather small  $J \sim 10$  it is already computationally demanding to identify all of the level crossings. As an example, Fig. 4(a) presents the typical level crossing behavior in the vicinity of a null eigenphase for  $J = 10$ . The Floquet states are seen to cross each other frequently, between different-parity states and between same-parity states. Both types of level crossings are of enormous interest. For the first type, at a crossing point an arbitrary superposition of two crossing states of different parities remains an eigenstate but generally breaks the parity symmetry, thereby maintaining a nonzero population difference between the two modes forever [13]. This makes it clear that the first type of level crossings give rise to the seminal CDT phenomenon [15] that has attracted broad experimental interests. Note that in some regimes of  $\hbar_\eta$ , to

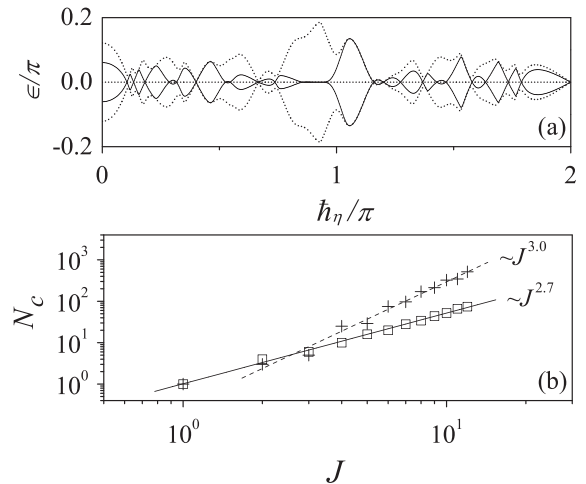


FIG. 4. (a) Level crossings between three even-parity states (dashed lines) and two odd-parity states (solid lines), for  $J = 10$  and  $\alpha/\hbar_{\text{eff}} = 1.0$ . (b) Number of level crossings versus  $J$ , for  $\hbar_\eta \in [0, 4\pi)$  and  $\alpha/\hbar_{\text{eff}} = 1.0$ . The cross (square) symbols are for crossings between different-parity (same-parity) states, and the fitting suggests a power law scaling  $J^{3.0}$  ( $J^{2.7}$ ).

the naked eye two curves of opposite parities in Fig. 4(a) are almost on top of each other, and as a result many CDT points are found in these regimes. Note also that CDT-induced population trapping is fundamentally different from the well-known self-trapping effect on the mean-field level. Indeed, the CDT effect here depends on  $\eta$  and  $J$ , whereas mean-field self-trapping is transient and independent of  $J$ . Now turning to the second type of level crossings, they come as a surprise because avoided crossings between same-parity states are generally anticipated for classically nonintegrable systems (see Fig. 2). The second type of crossings therefore suggest the uniqueness (e.g., some effective local “symmetry”) of  $F$  whose matrix elements in the  $|m\rangle$  representation are quasiperiodic. Recalling the above-mentioned extreme example where all levels cross at  $\hbar_\eta = 2\pi$  for integer  $J$ , we expect that special arithmetic properties of  $\hbar_\eta$  play a key role in both types of level crossings.

By obtaining all of the level crossings with high accuracy for  $J \leq 12$ , we obtain in Fig. 4(b) that the number of CDT points contained in the butterfly patterns scales as  $J^{3.0}$  and the number of same-parity crossings scales as  $J^{2.7}$ . In particular, we conclude that, as  $N$  goes to infinity, on average each pair of Floquet states in a butterfly pattern sees infinite CDT points.

In the kicked-Harper model, the quantization rule varies with the boundary condition adopted [20] and a compact toroidal phase space arises only if the Planck constant assumes special values [21]. A general treatment of the kicked-Harper model leads to a band structure that often complicates the issue. By contrast, the phase space here is necessarily on a sphere [18], with no arbitrariness in quantization and no band structure in the spectrum. For these reasons the new butterfly Floquet spectrum discovered in this work can stimulate more studies of the fractal Floquet spectrum in driven systems. Results here also suggest that our strategy in generating a butterfly quasienergy spectrum, namely, the use of partial cancellation of quasirandom phases (first advocated in a kicked-rotor system [5]), is widely applicable. Furthermore, it is now clear that three quantum chaos paradigms, i.e., the kicked-top, kicked-Harper, and kicked-rotor models, are all linked together for the first time, because all of them can display fractal statistics.

Finally, we mention two specific applications. First, because the found butterfly spectrum collapses at  $\hbar_\eta = 2\pi$  (or  $g_0 = \pi/4$ ) for integer  $J$ , one may experimentally determine if  $N$  is even or odd by scanning the dynamics in the neighborhood of  $g_0 = \pi/4$ . This possibility does not exist in the mean-field dynamics of a BEC. Similarly, one may study the CDT points to reveal non-mean-field effects. Second, it is now of great interest, both experimentally and computationally, to revisit early results of how a multifractal spectrum can be manifested in time-dependent properties [22].

Detailed results of this work will be published elsewhere [23]. We thank Professor C.-H. Lai for his encouragement. J. W. acknowledges support from DSTA of Singapore under Agreement No. POD0613356. J. G. is supported by WBS Grants No. R-144-050-193-101/133 and No. R-144-000-195-123.

\*phygj@nus.edu.sg

- [1] P. G. Harper, Proc. Phys. Soc. London Sect. A **68**, 874 (1955); D. R. Hofstadter, Phys. Rev. B **14**, 2239 (1976).
- [2] B. Simon, Commun. Math. Phys. **89**, 227 (1983); A. Avial and S. Jitomirskaya, arXiv:0503363 [Ann. Math. (to be published)].
- [3] For example, N. Goldman, Phys. Rev. A **77**, 053406 (2008); J. Phys. B **42**, 055302 (2009); for general interest in quantum phase transitions, see S. Sachdev, *Quantum Phase Transitions* (Cambridge University Press, Cambridge, England, 2000).
- [4] T. Geisel, R. Ketzmerick, and G. Petschel, Phys. Rev. Lett. **67**, 3635 (1991).
- [5] J. Wang and J. B. Gong, Phys. Rev. A **77**, 031405(R) (2008); J. Wang, A. S. Mouritzen, and J. B. Gong, J. Mod. Opt. **56**, 722 (2009).
- [6] D. W. Hone, R. Ketzmerick, and W. Kohn, Phys. Rev. A **56**, 4045 (1997).
- [7] R. Artuso, G. Casati, and D. Shepelyansky, Phys. Rev. Lett. **68**, 3826 (1992); R. Ketzmerick, G. Petschel, and T. Geisel, Phys. Rev. Lett. **69**, 695 (1992).
- [8] I. Dana, Phys. Lett. A **197**, 413 (1995).
- [9] I. Dana and D. L. Dorofeev, Phys. Rev. E **72**, 046205 (2005).
- [10] W. Lawton, A. S. Mouritzen, J. Wang, and J. B. Gong, J. Math. Phys. (N.Y.) **50**, 032103 (2009).
- [11] A. Eckardt, C. Weiss, and M. Holthaus, Phys. Rev. Lett. **95**, 260404 (2005); C. E. Creffield and T. S. Monteiro, Phys. Rev. Lett. **96**, 210403 (2006).
- [12] H. Lignier *et al.*, Phys. Rev. Lett. **99**, 220403 (2007); E. Kierig *et al.*, Phys. Rev. Lett. **100**, 190405 (2008).
- [13] M. P. Strzys, E. M. Graefe, and H. J. Korsch, New J. Phys. **10**, 013024 (2008).
- [14] Q. Zhang, P. Hänggi, and J. B. Gong, Phys. Rev. A **77**, 053607 (2008); New J. Phys. **10**, 073008 (2008).
- [15] F. Grossmann *et al.*, Phys. Rev. Lett. **67**, 516 (1991); V. G. Della Valle *et al.*, Phys. Rev. Lett. **98**, 263601 (2007); E. Kierig *et al.*, Phys. Rev. Lett. **100**, 190405 (2008).
- [16] G. J. Milburn *et al.*, Phys. Rev. A **55**, 4318 (1997).
- [17] J. Liu *et al.*, Phys. Rev. A **72**, 063623 (2005); Q. Xie and W. Hai, Eur. Phys. J. D **33**, 265 (2005).
- [18] F. Haake, *Quantum Signatures of Chaos* (Springer-Verlag, New York, 1992).
- [19] J. B. Gong and J. Wang, Phys. Rev. E **76**, 036217 (2007).
- [20] I. Guarneri and F. Borgonovi, J. Phys. A **26**, 119 (1993).
- [21] P. Leboeuf *et al.*, Phys. Rev. Lett. **65**, 3076 (1990).
- [22] I. Guarneri and G. Mantica, Phys. Rev. Lett. **73**, 3379 (1994); R. Ketzmerick *et al.*, *ibid.* **79**, 1959 (1997); F. Piéchon, *ibid.* **76**, 4372 (1996).
- [23] J. Wang and J. B. Gong, arXiv:0906.2257.